Chaotic Intrinsic Variability in the Arctic-North Atlantic Ocean and Its Link to Sea Ice

Camille Le Gloannec, Rym M'Sadek, Camille Lique, Éric Maisonnave, Claude Talandier, Thierry Penduff

AGU ADVANCING EARTH AND SPACE SCIENCES

Geophysical Research Letters

RESEARCH LETTER
10.1029/2024GL113318

Chaotic Intrinsic Variability in the Arctic-North Atlantic Ocean and Its Link to Sea Ice

C. Le Gloannec[1], R. Msadek[1], C. Lique[2], E. Maisonnave[1,3], C. Talandier[2], and T. Penduff[4]

[1]CECI, CNRS, CERFACS, Université de Toulouse, Toulouse, France, [2]Univ. Brest, CNRS, Ifremer, IRD, Laboratoire d'Océanographie Physique et Spatiale (LOPS), IUEM, Plouzané, France, [3]LOCEAN-IPSL, Sorbonne Université (UPMC)/IRD/CNRS/MNHN, UMR7159, Paris, France, [4]CNRS, IRD, Grenoble INP, INRAE, IGE, Université Grenoble Alpes, Grenoble, France

Key Points:

- Chaotic intrinsic variability greatly influences temperature variability in the northern North Atlantic in particular at the subsurface
- Salinity intrinsic variability is prominent in the Central Arctic, peaking in summer as sea ice cover decreases
- Enhanced horizontal gradients and variations in sea ice conditions favor the emergence of the ocean intrinsic variability in the Arctic

Supporting Information:

Supporting Information may be found in the online version of this article.

Correspondence to:

C. Le Gloannec,
legloannec@cerfacs.fr

Citation:

Le Gloannec, C., Msadek, R., Lique, C., Maisonnave, E., Talandier, C., & Penduff, T. (2025). Chaotic intrinsic variability in the Arctic-North Atlantic Ocean and its link to sea ice. *Geophysical Research Letters*, *52*, e2024GL113318. https://doi.org/10.1029/2024GL113318

Received 25 OCT 2024
Accepted 3 FEB 2025

Abstract We provide the first quantification of chaotic intrinsic variability (CIV) in the Arctic-North Atlantic region, using an ensemble of 13 eddy-permitting ocean–sea ice simulations. By isolating oceanic CIV from atmospheric variability, we show that CIV contributes 20%–60% of sea surface temperature interannual variability in the northern North Atlantic at the Arctic gateways, with a greater influence at subsurface levels. Salinity CIV accounts for 20%–50% of interannual variability, particularly in the Arctic. Furthermore, CIV contributes to a notable portion of sea ice concentration interannual variability in the marginal ice zone, likely influenced by dynamical interactions between sea ice and small-scale features. CIV is shown to emerge in preferential regions, with its seasonal amplitude modulated by sea ice conditions. Given the potential for CIV to amplify in a warming Arctic, understanding its role in ocean and sea ice variability under changing climate conditions is crucial for improving predictions in this region.

Plain Language Summary The Arctic Ocean is warming faster than the global average, leading to reduced and thinner sea ice, which no longer insulates the ocean as effectively. This change allows the ocean to respond more directly to both atmospheric variability and its own internal dynamics. Understanding these sources of variability is crucial for interpreting future changes in the Arctic. A key component of the ocean's internal variability is generated by mesoscale eddies, yet many current climate models do not fully capture these eddies, potentially overlooking important aspects of oceanic variability. In this study, we provide a detailed assessment of Arctic Ocean intrinsic variability using an ensemble of high-resolution simulations. Our analysis of the 2005–2015 period reveals that intrinsic ocean variability plays a significant role in interannual temperature variations in the northern North Atlantic, particularly at subsurface levels, while having a smaller impact in the central Arctic. Salinity variability is strongly influenced by ocean intrinsic variability, especially during the summer months when sea ice is melting. Our findings suggest that as the Arctic continues to warm, the influence of oceanic intrinsic variability is likely to intensify. This underscores the importance of better understanding small-scale ocean processes to improve climate projections for the Arctic.

1. Introduction

Arctic sea ice cover has decreased by approximately 55% in summer since the advent of satellite observations (e.g., Meier & Stroeve, 2022). This significant long-term decline is accompanied by notable year-to-year variability (Serreze et al., 2016), which is often viewed as a key source of uncertainty in future Arctic sea ice projections, as this variability can either mask or enhance the externally forced long-term trend (Swart et al., 2015). The interannual fluctuations affecting sea ice mainly stem from atmospheric drivers such as the Arctic Oscillation or its regional manifestation, the North Atlantic Oscillation (Deser et al., 2000; Thompson & Wallace, 1998). It is further shaped by the physical characteristics of Atlantic Waters, which flow into the Arctic Ocean via the Greenland and Norwegian seas (Årthun et al., 2012), and Pacific Waters, entering the Arctic through the Bering Strait (Woodgate, 2018). The presence of mesoscale eddies within these water masses can locally influence heat exchange and thus impact the formation and melting of sea ice (Cassianides et al., 2023; Von Appen et al., 2018). Further, the dynamics of the Arctic Ocean are distinct from those of mid-latitude regions, mostly due to the presence of sea ice and unique halocline stratification. Eddy-permitting ocean model simulations suggest that in the mid-latitudes, an important portion of ocean interannual variability also arises from chaotic intrinsic variability (CIV), which spontaneously emerges due to nonlinearities, irrespective of atmospheric variability (Leroux

et al., 2018; Llovel et al., 2018). However, the scale and spatial distribution of this intrinsic variability in the Arctic region, encompassing both ocean and sea ice variables remain largely unknown.

The level of mesoscale activity in the ice-covered Arctic remains largely uncertain, primarily due to observational challenges. Recent research, however, suggests a complex, mutual influence between mesoscale eddies and sea ice in the Arctic (Cassianides et al., 2023; Manucharyan & Thompson, 2022; Meneghello et al., 2021). Whether these interactions contribute to enhanced or reduced intrinsic variability in the region is yet to be determined. The interaction between ocean eddies and sea ice is multifaceted. On the one hand, studies have demonstrated that sea ice tends to dampen surface eddies in the Arctic, thereby restricting the development of nonlinearities when sea ice is densely packed (Meneghello et al., 2021). On the other hand, subsurface eddies located beneath the ice pack have been found to influence sea ice growth and melt (Cassianides et al., 2023). This indicates that CIV may be important in ice-covered regions below the sea surface, likely driven by the integrated effect of the dynamical interactions between sea ice and eddies.

In this study, we quantify the intrinsic interannual variability of ocean and sea ice in the Arctic-North Atlantic region. Our analysis is based on an ensemble of eddy-permitting regional ocean simulations, all driven by the same atmospheric forcing. Section 2 details the model configuration and the methodology used to quantify forced and intrinsic variability. The findings pertaining to surface and subsurface ocean and ice variables are presented in Sections 3.1 and 3.2. Section 3.3 delves into the potential mechanisms underlying ocean intrinsic variability, while the final conclusions are summarized in Section 4.

2. Model Description and Methodology

The current study is based on 13 ocean-sea ice simulations conducted using a regional Arctic-North Atlantic model configuration (CREG12, Canadian REGional; Dupont et al., 2015), which utilizes NEMO 3.6 (Nucleus for European Modeling of the Ocean, Madec et al., 2017) for the ocean component, and LIM 3.5 (Louvain-La-Neuve sea Ice Model, Rousset et al., 2015) for the sea ice component. The model configuration features a high horizontal resolution ($^1/_{12}°$, equivalent to 3–4 km in the Arctic) and a fine vertical resolution (75 levels, spacing from 1 m at the surface to 20 m at 200 m depth). The simulations are forced by atmospheric conditions from DFS 5.2 (Drakkar Forcing Set, Dussin et al., 2018), a data set derived from ERA-40 and ERA-Interim reanalyses. Along the lateral open boundaries, monthly mean conditions (comprising 3D velocities, temperature, salinity, sea ice thickness and concentration) taken from a global ORCA12 simulation are applied (Treguier et al., 2017). Following the probabilistic methodology outlined by Penduff et al. (2014), the 13 ensemble members were initialized from a single spin-up simulation that covered the period from 1979 to 2014. The ensemble spread was generated by introducing a stochastic perturbation to the density equation in the NEMO ocean code, which was applied for one year in 2005 (Brankart et al., 2015). After initiating the perturbation, it takes approximately a year to develop and stabilize (see Figures S8 and S9 in Supporting Information S1). Therefore, we exclude the first year from our analysis and focus on the remaining 2006–2014 period. More details about the numerical design as well as the representation of the mesoscale activity in the Arctic Basin in the longer simulation can be found in Regan et al. (2020) and in Supporting Information (Figures S1 and S2 along with Text S2 in Supporting Information S1).

In the subsequent analyses, we quantify the interannual intrinsic and forced variability using 5-day mean model outputs that have been linearly detrended and deseasonalized at each grid point and for each member before the calculations in order to remove both the imprint of lower frequency variability (linear trend) and the seasonal variation component (mean seasonal cycle).

Following Leroux et al. (2018) and Hogg et al. (2022), the atmospherically forced component, shared among all members, is defined as the ensemble mean $\langle f_i(t)\rangle$, where $f_i(t)$ represents the time series of any variable at a given location for each member i. The CIV component is defined as the ensemble standard deviation $\epsilon(f_i(t))$. The magnitude of the forced variability is computed as the temporal standard deviation of the ensemble mean, denoted as $A_{\text{forced}} = \sigma(\langle f_i(t)\rangle)$, while the magnitude of the intrinsic variability is computed as the square-root of the time mean of the ensemble variance expressed as $A_{\text{intrinsic}} = \sqrt{\overline{\epsilon^2(f_i(t))}}$. The total variability amplitude is subsequently estimated as the square-root of the ensemble mean of the time variance given by $A_{\text{total}} = \sqrt{\overline{\sigma^2(f_i(t))}}$. These three quantities are linked by the relation $A^2_{\text{total}} = A^2_{\text{forced}} + A^2_{\text{intrinsic}}$. Note that we use the biased estimate of the variance and we linearly detrend each member; hence there is no residual in the above decomposition

(Hogg et al., 2022). Finally, in order to discuss the relative contribution of the intrinsic component to the total variability, we define $R = \frac{A_{\text{intrinsic}}}{A_{\text{total}}}$. The complete derivation of the intrinsic, forced and total variability is provided in Supporting Information (Text S1 in Supporting Information S1).

3. Results

3.1. Signature of the Intrinsic Interannual Variability on Surface and Subsurface Temperature in the Arctic-North Atlantic Region

Over the 2006–2014 period, interannual CIV exerts a notable influence on sea surface temperature (SST) in the Arctic-North Atlantic region, with greater magnitudes simulated in the northern North Atlantic compared to the Arctic (Figure 1a). Although atmospheric-driven variability predominantly governs most of the Arctic's SST interannual variability (Figure 1b), CIV still accounts for 20%–50% of the total variability in the Nansen Basin and in a small part of the Amundsen Basin north of the Laptev Sea. Moreover, it exceeds forced variability in the Greenland, Iceland and Norwegian (GIN) seas as well as in the Labrador Current where values can reach up to 1°C (Figure 1a). The contribution of CIV increases with depth. At 200 m depth — which is below the mixed layer except in regions of deep convection—, intrinsic variability accounts for more than 50% of the total temperature variability across much of the northern North Atlantic basin, with localized values exceeding 1.5°C. This amplification with depth is also evident in the Arctic, albeit with a more confined influence, predominantly in the Eurasian Basin and over the continental slope, where Atlantic Water is primarily advected by the mean flow (Figures 1c and 1d). The stronger impact of intrinsic variability in the subsurface aligns with reduced influence of the atmospheric forcing beneath the surface and sustained eddy activity throughout the seasons, consistent with findings reported by Meneghello et al. (2021).

While the average magnitude of interannual temperature intrinsic variability remains around 1°C over the 2006–2014 period for a typical location in the northern North Atlantic, it can increase significantly in some years, reaching up to 40% higher (see Figures S8 and S9 along with Text S5 in Supporting Information S1). This highlights the substantial year-to-year variability of CIV in this region. Additionally, CIV may show localized increases when analyzed at a specific grid point, rather than when averaged over a larger area, consistent with the tendency for individual eddies to be smoothed out at broader scales. In deep convection regions such as the Labrador Sea and the GIN seas, CIV undergoes a seasonal intensification during winter (January–February–March, JFM in the following), likely associated with convective instability. To gain a deeper insight into the seasonality of CIV in the Arctic region, our focus now shifts to examining the influence of seasonal sea ice cover on oceanic intrinsic variability.

3.2. Connecting Intrinsic Interannual Variability of Sea Surface Salinity to Sea Ice Cover

Sea ice cover is strongly coupled to SST during its formation, as colder temperatures facilitate the freezing of seawater. Several observational and modeling studies have also demonstrated the importance of salinity in regulating sea ice growth and decay by affecting the freezing point of seawater and its buoyancy characteristics (e.g., Feltham et al., 2006). The link between sea ice conditions and salinity is actually twofold. The seasonal fluctuations in sea ice conditions in the Arctic substantially influence salinity through processes like brine rejection during sea ice formation, freshwater input from melting ice, and changes in vertical mixing. Consequently, it is not surprising that the influence of interannual sea surface salinity (SSS) CIV during contrasted seasons in the Arctic is strongly tied to the seasonal variability of sea ice concentration. Further, in the Arctic, variations in salinity play a key role in setting the density, which in turn greatly influences geostrophy and stratification. Understanding the drivers of salinity variability in this region is therefore crucial.

As illustrated in Figure 2, there is a significant imprint of CIV on SSS in the North Atlantic-Arctic region, particularly in the marginal ice zone (MIZ, where sea ice concentration is between 0.15 and 0.80, e.g., Rolph et al., 2020) and along the strong currents in the Arctic corridor, such as the East Greenland Current and Labrador Current. In these areas, during the 2006–2014 period, CIV reaches up to 0.4 psu in winter (JFM) and 0.6 psu in summer (July–August–September, JAS in the following), exceeding 20% of the total variability in all cases. Additionally, enhanced SSS CIV, accounting for between 20% and 50% of the total interannual variability, is also simulated in the Eurasian Basin along major topographic features such as the Lomonosov and Gakkel ridges. Although this region belongs to the sea ice pack in winter, CIV persists throughout winter. Notably, the magnitude

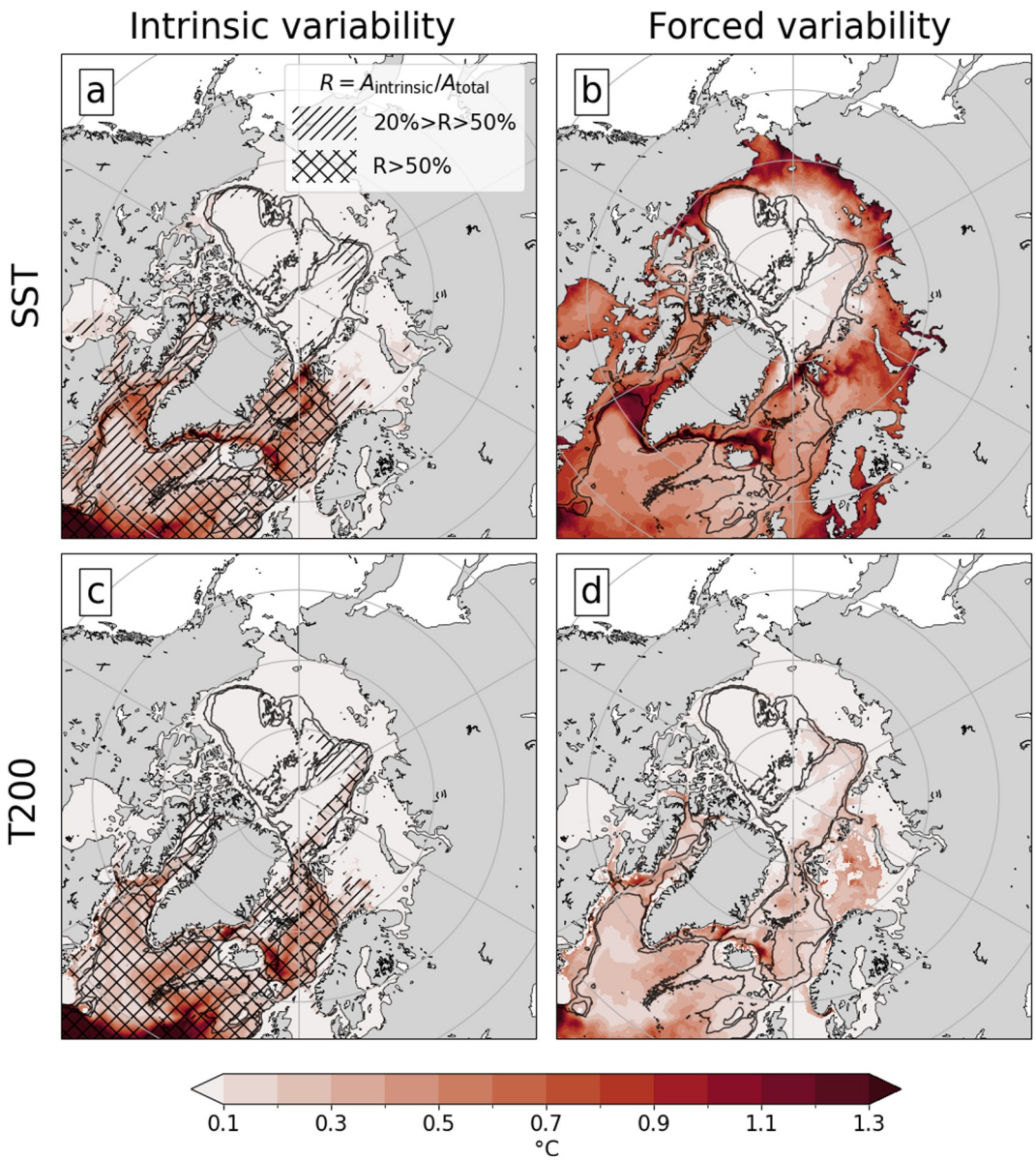

Figure 1. Maps of interannual intrinsic and forced variability ($A_{intrinsic}$ and A_{forced} as defined in Section 2) for annual (a, b) sea surface temperature and (c, d) temperature at 200 m depth computed from 5-day mean outputs over the 2006–2014 period. Hatched regions in panels (a, c) indicate areas where $20\% < R < 50\%$, while dotted regions denote areas where $R > 50\%$. Note that the ratio is computed only in regions where the total variability exceeds 0.1°C. The black contours indicate the 500 and 2,000 m isobaths.

of SSS CIV is greater in JAS/summer than in JFM/winter, and it exhibits a coincidence with the position of the MIZ over most of the Eurasian Basin and north of the Canadian coast (Figures 2a and 2c). This aligns with the enhanced influence of surface eddies during JAS/summer in ice-covered areas, when sea ice concentration decreases (Manucharyan & Thompson, 2022). In JFM/winter, eddies are more likely to be dissipated by sea ice friction, resulting in a diminished impact of eddies on both sea ice and the ocean surface. We observe that in regions such as the Kara Sea, Baffin Bay, and Hudson Bay, where sea ice is less consolidated (below 0.8 concentration) and thinner in JAS/summer compared to JFM/winter, SSS CIV is intensified during JAS/summer compared to JFM/winter. Indeed, previous studies have shown that ocean kinetic energy and momentum input are significantly dampened when sea ice concentration exceeds 0.8 (e.g., Manucharyan & Thompson, 2022; Martin

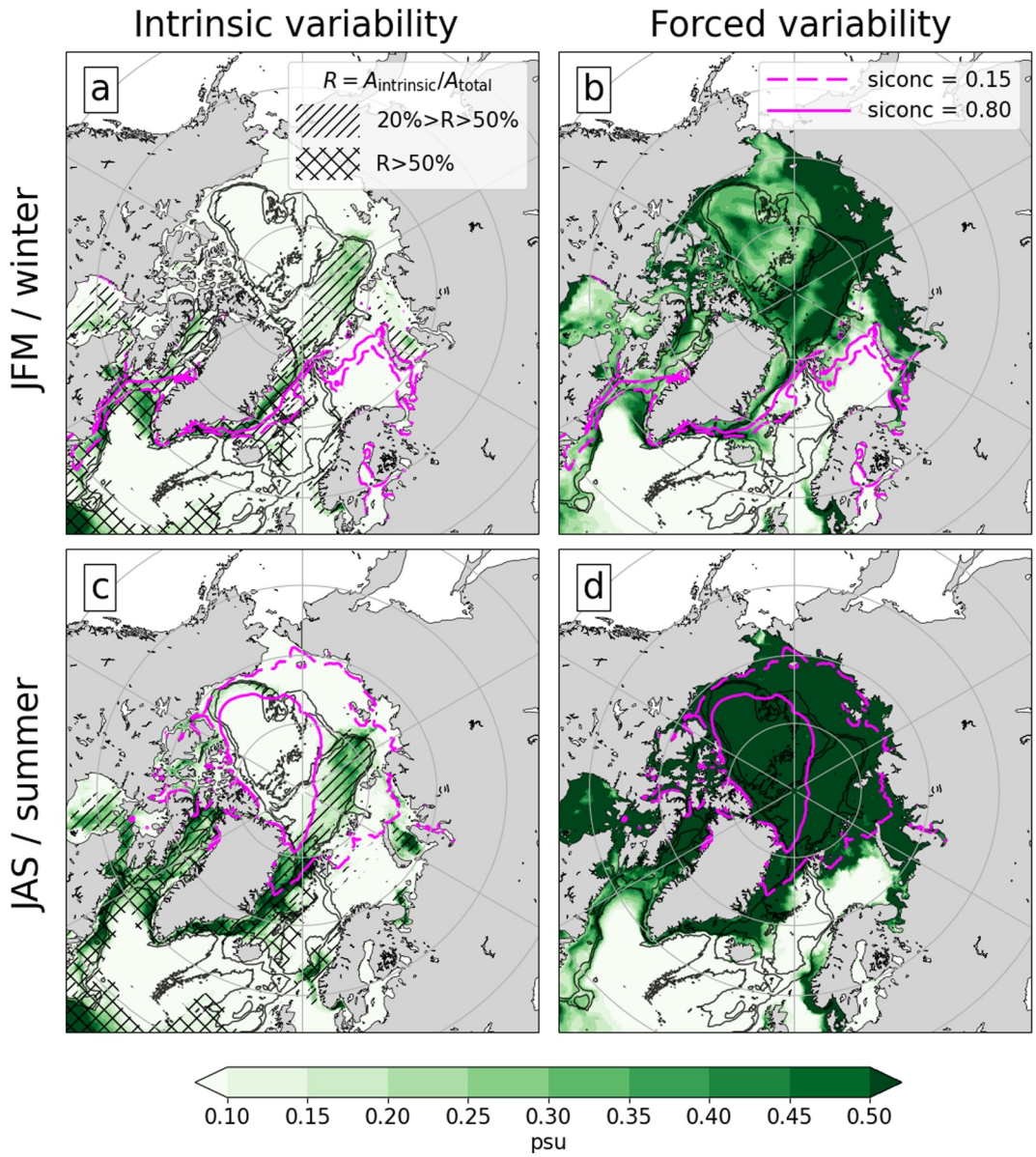

Figure 2. Maps of interannual intrinsic and forced variability ($A_{intrinsic}$ and A_{forced} as defined in Section 2) for sea surface salinity during (a, b) winter (JFM: January–February–March) and (c, d) summer (JAS: July–August–September) computed from 5-day mean outputs over the 2006–2014 period. Contours showing 0.15 (dashed pink) and 0.80 (solid pink) sea ice concentration correspond to the ensemble mean. Hatched regions in panels (a, c) indicate areas where $20\% < R < 50\%$, while cross hatched regions denote areas where $R > 50\%$. Note that the ratio is computed only in regions where the total variability exceeds 0.1 psu. The black contours indicate the 500 and 2,000 m isobaths.

et al., 2014). In contrast, the temperature CIV does not exhibit such distinct seasonal patterns (see Figures S5 and S6 in Supporting Information S1).

This contrast in intrinsic variability between the compact sea ice pack and the MIZ becomes more pronounced when examining sea ice concentration CIV (Figure 3). During JFM/winter, CIV peaks at 0.1 in the MIZ, while remaining nearly absent within the ice pack. Meanwhile, the forced atmospheric contribution reaches up to 0.06 within the ice pack and exceeds 0.3 in the MIZ. In JAS/summer, the MIZ expansion leads to more distinct patterns of sea ice concentration CIV, exhibiting notable similarities in spatial patterns with SSS CIV (see Figure 2), related to sea ice melt and formation (see Text S4 and Figure S7 in Supporting Information S1). Note that the sea ice concentration CIV never exceeds 50% of the total variability (not shown).

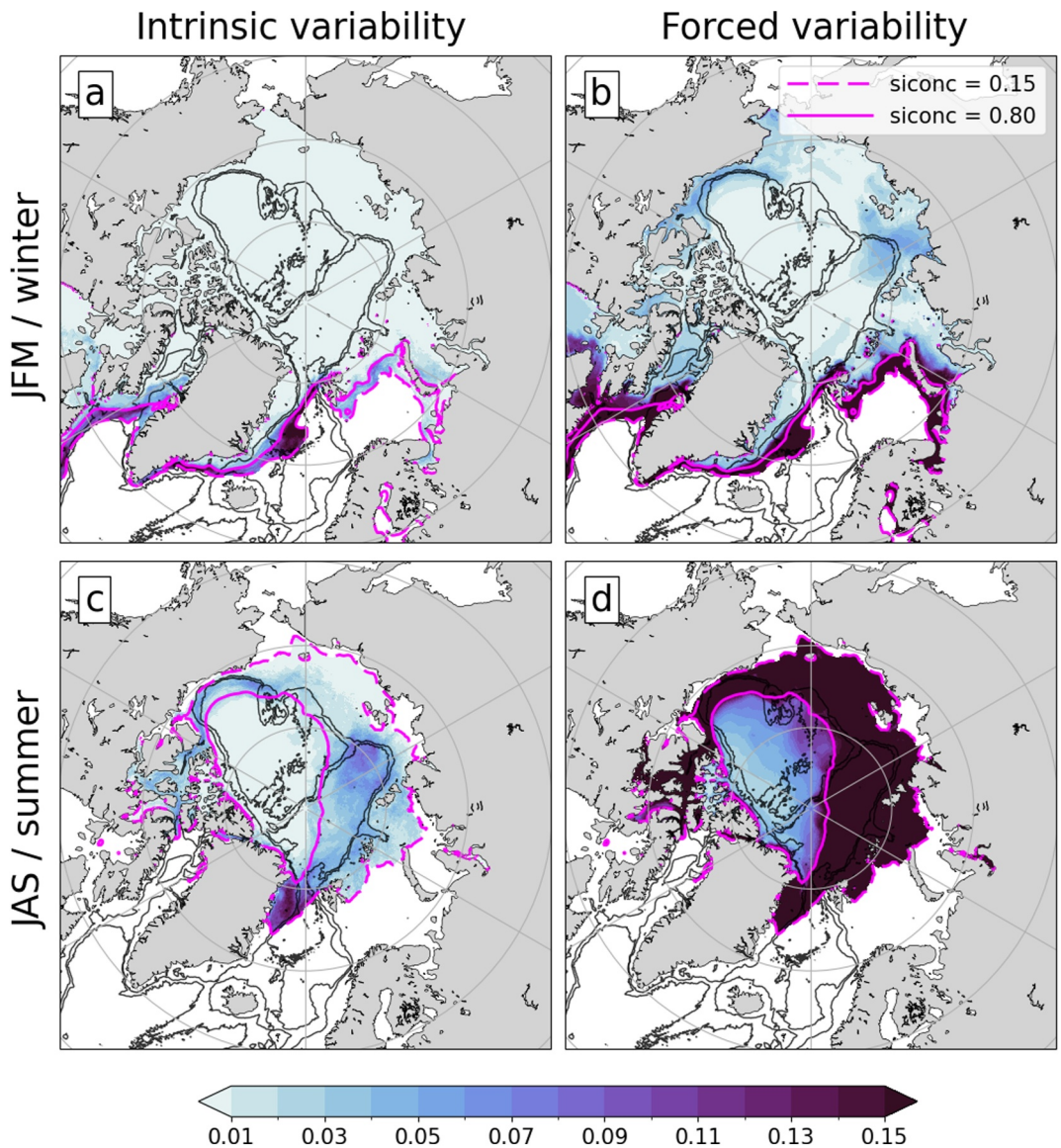

Figure 3. Same as Figure 2 but for sea ice concentration. Note that to prevent bias in the results due to grid points with very low sea ice concentration, we restricted our analysis to grid points where at least 6 out of the 13 members have a sea ice concentration value exceeding 0.15 over the season of interest.

3.3. Sources of Intrinsic Interannual Variability in the Arctic-North Atlantic Region

Our findings reveal varied patterns of intrinsic variability depending on the specific variable examined, suggesting distinct processes favoring the emergence of ocean and sea ice intrinsic variability. In this section, we delve into the physical processes that could explain the spatio-temporal structure of intrinsic variability in the Arctic region. The highest values of SST and SSS CIV coincide with areas of intensified SST and SSS gradients in the North Atlantic-Arctic region (Figures 4a–4c). Specifically, in the northern North Atlantic, average SST and SSS gradients over the 2006–2014 period reach values as high as 8°C/100 km and 5 psu/100 km, respectively, particularly along the main boundary currents and in the MIZ, due to complex bathymetry. These regions align with the areas of maximum SST and SSS CIV described earlier (Figures 1 and 2). The CIV in these regions likely arises from pronounced thermohaline variations and spatial gradients in frontal currents. Moreover, areas with enhanced density gradients are hotspots for instabilities and the preferential generation of mesoscale features. Notably, the regions of maximum SST and SSS CIV also coincide with areas of enhanced surface eddy kinetic energy in the Arctic, as shown in Figure S1 in Supporting Information S1.

10.1029/2024GL113318

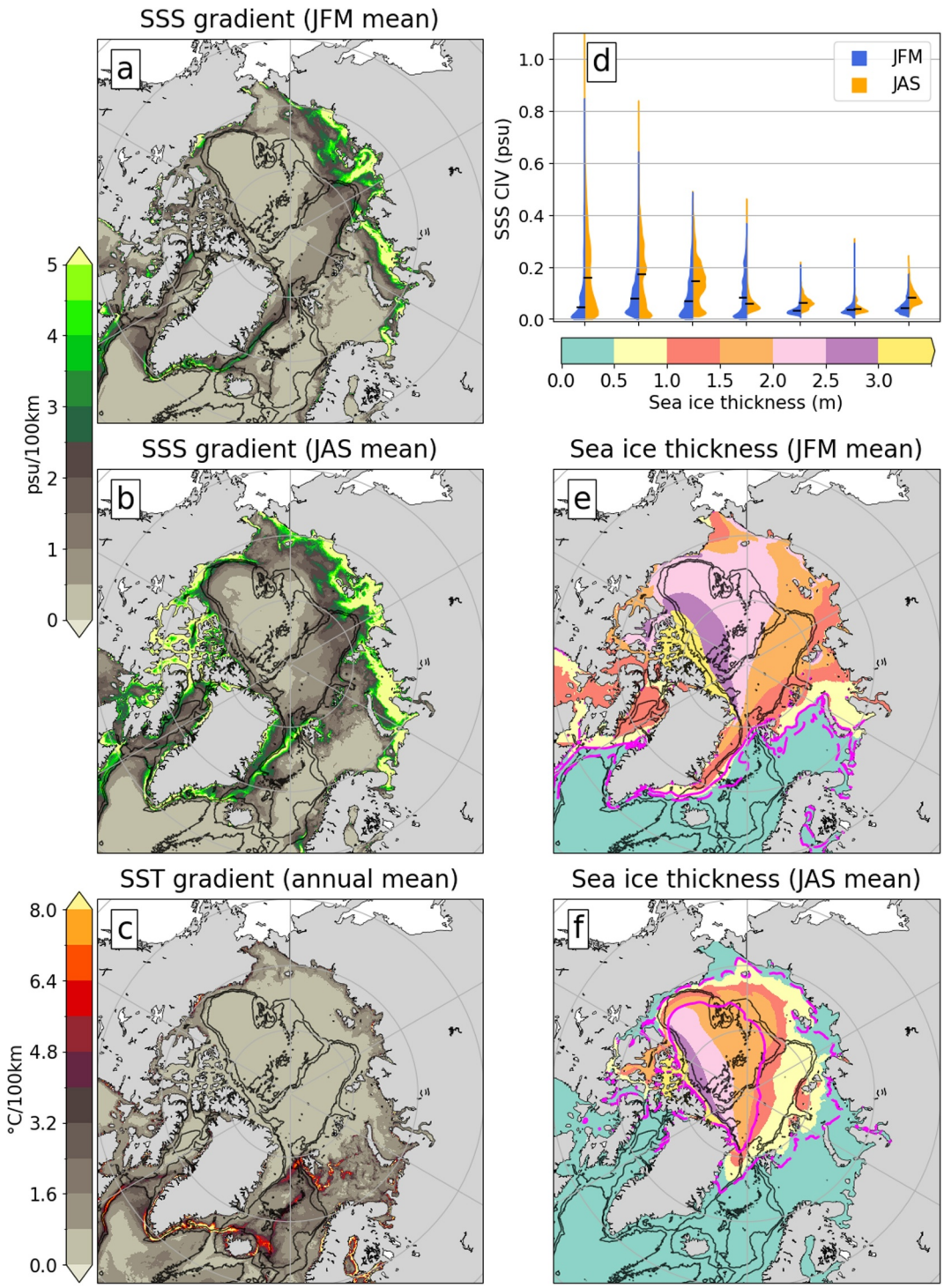

Figure 4. Maps of the ensemble mean of (a) JFM sea surface salinity (SSS) gradient, and (b) JAS SSS gradient and (c) annual sea surface temperature gradient, computed from 5-day mean outputs averaged over the 2006–2014 period. The black contours indicate the 500 and 2,000 m isobaths. Panel (d) presents violin plots showing the distribution of SSS chaotic intrinsic variability by sea ice thickness classes for JFM/winter (blue) and JAS/summer (orange). The black dash shows the median of each distribution. Regions corresponding to each sea ice thickness classes are shown on (e, f).

However, large values of SSS gradients do not always result in increased CIV, as evidenced by the elevated gradient near the shelf within the Arctic Basin, which is linked to freezing and melting processes and possibly large river runoff, but does not coincide with significant SSS CIV. This discrepancy may be due to the fact that eddies are not resolved in these shallow regions due to our 4 km resolution. Another hypothesis is that the pattern of SSS CIV may not be solely driven by strong gradients, but is rather more closely associated with variability in sea ice conditions.

To further evaluate the relationship between SSS CIV and sea ice thickness, we analyze its distribution over the period 2006–2014 (Figure 4d). This reveals that thinner sea ice is associated with higher values of SSS CIV. Specifically, SSS CIV does not exceed 0.4 psu when sea ice thickness is greater than 2 m. This supports our previous finding that SSS CIV is generally higher in JAS/summer than in JFM/winter, with one exception: the 1.5–2.0 m sea ice thickness range, which is primarily associated with the Eurasian Basin in JFM/winter (Figure 4e), where SSS CIV persists (Figure 2a), and the Canadian Basin in JAS/summer (Figure 4f), where SSS CIV is minimal (Figure 2c). Relatively high extreme values of SSS CIV stand out in the lowest sea ice thickness ranges (Figure 4d). For the 0–0.5 m range, corresponding to the MIZ and ice edge (Figure 4e) in JFM/winter, SSS CIV peaks at 0.8 psu, highlighting the influence of the East Greenland and Labrador currents identified in Figure 2a. In JAS/summer, SSS CIV can exceed 1 psu in the 0–0.5 m range, corresponding primarily to open ocean regions (Figure 4f), including the Kara Sea, as well as the East Greenland and Labrador current regions, which were identified as areas of high SSS CIV in Figure 2c.

4. Conclusion

This study provides the first description of the influence of CIV on the seasonal to interannual variability of the ocean and sea ice in the Arctic-North Atlantic region. Using a novel ensemble of 13 ocean-sea ice eddy-permitting simulations, we successfully isolated oceanic and sea ice CIV from atmospherically forced variability.

Our findings reveal that in the northern North Atlantic, interannual CIV is a major contributor to SST variability, accounting for 20%–60% of the total variability and even dominating at subsurface levels. Notably, temperature CIV is significantly weaker in ice-covered regions, manifesting only in areas with enhanced gradients, highlighting a key spatial distinction in CIV behavior.

In contrast, we observe a notable salinity interannual CIV within the Arctic Basin and along its margins, intricately linked to seasonal fluctuations of the sea ice conditions. SSS CIV accounts for 20%–50% of the total interannual variability in the Eurasian Basin and exceeds 50% in the Atlantic Sector of the Arctic. It is more pronounced in summer than in winter, reflecting the increased activity of surface eddies as sea ice extent diminishes. Interestingly, while extensive sea ice cover may dissipate surface eddies in winter, CIV does not disappear uniformly across all regions. Instead, it emerges in preferential locations, influenced by bathymetry, and can persist through winter. Subsurface eddies may continue to generate CIV at depth, and the formation of sea ice itself may also contribute to the emergence of SSS CIV. Crucially, we find that interannual CIV in sea ice concentration is exclusively detected within the MIZ, where sea ice is less consolidated, and eddy activity is intensified. This is a critical insight into the dynamical interplay between sea ice and ocean variability.

We identify several potential mechanisms that favor the emergence of interannual CIV in specific regions of the Arctic-North Atlantic. These include enhanced horizontal density gradients, found in boundary current regions, topographically complex areas, and locations with significant freshwater input such as the sea ice edge, as well as varying sea ice conditions, favoring the emergence of CIV.

Interestingly, our study did not detect any significant CIV in the Canadian Basin, despite the energetic eddy field associated with the Beaufort Gyre (Regan et al., 2020; Timmermans & Marshall, 2020). This absence could reflect the lack of strong thermohaline anomalies carried by the mesoscale eddies formed in the interior of the Beaufort Gyre.

Beyond the Canadian Basin, our results may be limited by the horizontal resolution of our simulations. Indeed, the model is eddy permitting in most of the Arctic Ocean, even eddy-resolving in the central Arctic, but does not resolve eddies on the shelves (see Text S2 and Figure S2 in Supporting Information S1). Hence in these regions, the imprint of the CIV is very likely underestimated. Moreover, based on the analysis of a model run at 1 km, Liu et al. (2024) found that the surface kinetic energy content is the highest in the scale band of 1–10 km. Further, Wang et al. (2020) showed that increasing the model resolution from 4 to 1 km increases the Arctic EKE by 40%.

Further, we acknowledge that the design of our simulations-specifically, the use of a bulk formula for surface forcing, which introduces member-specific variations - may lead to an underestimation of surface CIV as suggested by Narinc et al. (2024).

Looking forward, our findings underscore the potential for CIV to have an increasingly significant impact in the context of a warming climate. With the Arctic projected to transition to a seasonally ice-free state in the coming decades (Haine & Martin, 2017), where summer ice-free conditions and thinner winter sea ice prevail, we anticipate a more pronounced effect of CIV on ocean variability, consistent with predictions of enhanced eddy activity in a warmer climate (Li et al., 2024). Additionally, our research suggests that temperature CIV, currently linked to the propagation of Atlantic Water, could expand its influence within the Arctic Basin as a result of the ongoing Atlantification of the Arctic Ocean. These insights are urging us to further improve the characterization and understanding of CIV across varying climate states, particularly in the rapidly changing Arctic environment.

Finally, we highlight that while many recent studies have examined the influence of internal atmospheric variability on Arctic sea ice cover (Dörr et al., 2023; Swart et al., 2015; Van Achter et al., 2020), our work takes a complementary approach by quantifying the contribution of oceanic internal variability associated with mesoscale features in this region. This perspective adds to the growing understanding of the complex interactions shaping Arctic sea ice dynamics and builds upon the insights of previous studies.

Data Availability Statement

Python and NCL were used for all analyses. Post-processing codes, post-processed model output, and the code used to produce the figures are available on Zenodo (Le Gloannec, 2024).

Acknowledgments
This work was supported by the INSU-LEFE program as part of the ICARE project. This research is also supported by the SASIP project funded by Schmidt Sciences—a philanthropic initiative that seeks to improve societal outcomes through the development of emerging science and technologies (Grant 353). This study contributed to the CLIMArcTIC project funded by the "PPR Océan et Climat—France 2030" (contract ANR-22-POCE-0005). We thank Giovanni Rugiero and Gilles Garric at Mercator for useful discussions at the start of the project. We also thank Laurent Terray for his help in designing the figures. Finally we thank the two anonymous reviewers for their constructive comments and suggestions that allowed us to improve the manuscript.

References

Årthun, M., Eldevik, T., Smedsrud, L. H., Skagseth, Ø., & Ingvaldsen, R. B. (2012). Quantifying the influence of Atlantic heat on Barents sea ice variability and retreat. *Journal of Climate*, *25*(13), 4736–4743. https://doi.org/10.1175/JCLI-D-11-00466.1

Brankart, J.-M., Candille, G., Garnier, F., Calone, C., Melet, A., Bouttier, P.-A., et al. (2015). A generic approach to explicit simulation of uncertainty in the NEMO ocean model. *Geoscientific Model Development*, *8*(5), 1285–1297. https://doi.org/10.5194/gmd-8-1285-2015

Cassianides, A., Lique, C., Tréguier, A., Meneghello, G., & De Marez, C. (2023). Observed spatio-temporal variability of the eddy-sea ice interactions in the Arctic Basin. *Journal of Geophysical Research: Oceans*, *128*(6), e2022JC019469. https://doi.org/10.1029/2022JC019469

Deser, C., Walsh, J. E., & Timlin, M. S. (2000). Arctic Sea ice variability in the context of recent atmospheric circulation trends. *Journal of Climate*, *13*(3), 617–633. https://doi.org/10.1175/1520-0442(2000)013⟨0617:ASIVIT⟩2.0.CO;2

Dörr, J. S., Bonan, D. B., Årthun, M., Svendsen, L., & Wills, R. C. J. (2023). Forced and internal components of observed Arctic sea-ice changes. *The Cryosphere*, *17*(9), 4133–4153. https://doi.org/10.5194/tc-17-4133-2023

Dupont, F., Higginson, S., Bourdallé-Badie, R., Lu, Y., Roy, F., Smith, G. C., et al. (2015). A high-resolution ocean and sea-ice modelling system for the Arctic and North Atlantic oceans. *Geoscientific Model Development*, *8*(5), 1577–1594. https://doi.org/10.5194/gmd-8-1577-2015

Dussin, R., Barnier, B., Brodeau, L., & Molines, J.-M. (2018). *The making of the Drakkar forcing set Dfs5* (Tech. Rep.). Zenodo. https://doi.org/10.5281/ZENODO.1209243

Feltham, D. L., Untersteiner, N., Wettlaufer, J. S., & Worster, M. G. (2006). Sea ice is a mushy layer. *Geophysical Research Letters*, *33*(14), 2006GL026290. https://doi.org/10.1029/2006GL026290

Haine, T. W. N., & Martin, T. (2017). The Arctic-Subarctic sea ice system is entering a seasonal regime: Implications for future Arctic amplification. *Scientific Reports*, *7*(1), 4618. https://doi.org/10.1038/s41598-017-04573-0

Hogg, A. M., Penduff, T., Close, S. E., Dewar, W. K., Constantinou, N. C., & Martínez-Moreno, J. (2022). Circumpolar variations in the chaotic nature of Southern Ocean eddy dynamics. *Journal of Geophysical Research: Oceans*, *127*(5), e2022JC018440. https://doi.org/10.1029/2022JC018440

Le Gloannec, C. (2024). Chaotic intrinsic variability in the arctic-north Atlantic and its link to sea ice [Collection]. *Zenodo*. https://doi.org/10.5281/zenodo.14645635

Leroux, S., Penduff, T., Bessières, L., Molines, J.-M., Brankart, J.-M., Sérazin, G., et al. (2018). Intrinsic and atmospherically forced variability of the AMOC: Insights from a large-ensemble ocean hindcast. *Journal of Climate*, *31*(3), 1183–1203. https://doi.org/10.1175/JCLI-D-17-0168.1

Li, X., Wang, Q., Danilov, S., Koldunov, N., Liu, C., Müller, V., et al. (2024). Eddy activity in the Arctic Ocean projected to surge in a warming world. *Nature Climate Change*, *14*(2), 156–162. https://doi.org/10.1038/s41558-023-01908-w

Liu, C., Wang, Q., Danilov, S., Koldunov, N., Müller, V., Li, X., et al. (2024). Spatial scales of kinetic energy in the Arctic Ocean. *Journal of Geophysical Research: Oceans*, *129*(3), e2023JC020013. https://doi.org/10.1029/2023JC020013

Llovel, W., Penduff, T., Meyssignac, B., Molines, J., Terray, L., Bessières, L., & Barnier, B. (2018). Contributions of atmospheric forcing and chaotic ocean variability to regional sea level trends over 1993–2015. *Geophysical Research Letters*, *45*(24). https://doi.org/10.1029/2018GL080838

Madec, G., Bourdallé-Badie, R., Pierre-Antoine, B., Bricaud, C., Bruciaferri, D., Calvert, D., et al. (2017). NEMO ocean engine. Version Number: v3.6-patch. *Zenodo*. https://doi.org/10.5281/ZENODO.3248739

Manucharyan, G. E., & Thompson, A. F. (2022). Heavy footprints of upper-ocean eddies on weakened Arctic sea ice in marginal ice zones. *Nature Communications*, *13*(1), 2147. https://doi.org/10.1038/s41467-022-29663-0

Martin, T., Steele, M., & Zhang, J. (2014). Seasonality and long-term trend of Arctic Ocean surface stress in a model. *Journal of Geophysical Research: Oceans*, *119*(3), 1723–1738. https://doi.org/10.1002/2013JC009425

Meier, W., & Stroeve, J. (2022). An updated assessment of the changing Arctic sea ice cover. *Oceanography*. https://doi.org/10.5670/oceanog.2022.114

Meneghello, G., Marshall, J., Lique, C., Isachsen, P. E., Doddridge, E., Campin, J.-M., et al. (2021). Genesis and decay of mesoscale baroclinic eddies in the seasonally ice-covered interior Arctic Ocean. *Journal of Physical Oceanography*, *51*(1), 115–129. https://doi.org/10.1175/JPO-D-20-0054.1

Narinc, O., Penduff, T., Maze, G., Leroux, S., & Molines, J.-M. (2024). North Atlantic Subtropical Mode Water properties: Intrinsic and atmospherically-forced interannual variability. https://doi.org/10.5194/egusphere-2024-1146

Penduff, T., Barnier, B., Terray, L., Sérazin, G., Gregorio, S., Brankart, J.-M., et al. (2014). Ensembles of eddying ocean simulations for climate. CLIVAR Exchanges No. 65, 19, 26.

Regan, H., Lique, C., Talandier, C., & Meneghello, G. (2020). Response of total and eddy kinetic energy to the recent spinup of the Beaufort Gyre. *Journal of Physical Oceanography*, *50*(3), 575–594. https://doi.org/10.1175/JPO-D-19-0234.1

Rolph, R. J., Feltham, D. L., & Schröder, D. (2020). Changes of the Arctic marginal ice zone during the satellite era. *The Cryosphere*, *14*(6), 1971–1984. https://doi.org/10.5194/tc-14-1971-2020

Rousset, C., Vancoppenolle, M., Madec, G., Fichefet, T., Flavoni, S., Barthélemy, A., et al. (2015). The Louvain-la-Neuve sea ice model LIM3.5: Global and regional capabilities. https://doi.org/10.5194/gmdd-8-3403-2015

Serreze, M. C., Crawford, A. D., Stroeve, J. C., Barrett, A. P., & Woodgate, R. A. (2016). Variability, trends, and predictability of seasonal sea ice retreat and advance in the Chukchi Sea. *Journal of Geophysical Research: Oceans*, *121*(10), 7308–7325. https://doi.org/10.1002/2016JC011977

Swart, N. C., Fyfe, J. C., Hawkins, E., Kay, J. E., & Jahn, A. (2015). Influence of internal variability on Arctic sea-ice trends. *Nature Climate Change*, *5*(2), 86–89. https://doi.org/10.1038/nclimate2483

Thompson, D. W. J., & Wallace, J. M. (1998). The Arctic oscillation signature in the wintertime geopotential height and temperature fields. *Geophysical Research Letters*, *25*(9), 1297–1300. https://doi.org/10.1029/98GL00950

Timmermans, M., & Marshall, J. (2020). Understanding Arctic Ocean circulation: A review of ocean dynamics in a changing climate. *Journal of Geophysical Research: Oceans*, *125*(4), e2018JC014378. https://doi.org/10.1029/2018JC014378

Treguier, A. M., Lique, C., Deshayes, J., & Molines, J. M. (2017). The North Atlantic eddy heat transport and its relation with the vertical tilting of the gulf stream axis. *Journal of Physical Oceanography*, *47*(6), 1281–1289. https://doi.org/10.1175/JPO-D-16-0172.1

Van Achter, G., Ponsoni, L., Massonnet, F., Fichefet, T., & Legat, V. (2020). Brief communication: Arctic sea ice thickness internal variability and its changes under historical and anthropogenic forcing. *The Cryosphere*, *14*(10), 3479–3486. https://doi.org/10.5194/tc-14-3479-2020

Von Appen, W., Wekerle, C., Hehemann, L., Schourup-Kristensen, V., Konrad, C., & Iversen, M. H. (2018). Observations of a submesoscale cyclonic filament in the marginal ice zone. *Geophysical Research Letters*, *45*(12), 6141–6149. https://doi.org/10.1029/2018GL077897

Wang, Q., Koldunov, N. V., Danilov, S., Sidorenko, D., Wekerle, C., Scholz, P., et al. (2020). Eddy kinetic energy in the Arctic Ocean from a global simulation with a 1-km arctic. *Geophysical Research Letters*, *47*(14), e2020GL088550. https://doi.org/10.1029/2020GL088550

Woodgate, R. A. (2018). Increases in the Pacific inflow to the Arctic from 1990 to 2015, and insights into seasonal trends and driving mechanisms from year-round Bering Strait mooring data. *Progress in Oceanography*, *160*, 124–154. https://doi.org/10.1016/j.pocean.2017.12.007